Title: EigenGWAS: finding loci under selection through genome-wide association studies of eigenvectors in structured populations

Authors: Guo-Bo Chen[1], Sang Hong Lee[1,2], Zhi-Xiang Zhu[3], Beben Benyamin[1], Matthew R. Robinson[1]

Affiliation:
[1]Queensland Brain Institute, The University of Queensland, Brisbane, QLD 4072, Australia; [2]School of Environmental and Rural Science, The University of New England, Armidale, NSW 2351, Australia; [3]SPLUS Game, Guangzhou, Guangdong 510665, China

Running Title: EigenGWAS for selection

Keywords: GWAS, Eigenvector, selection, population structure

Correspondence should be addressed to
GBC (chen.guobo@foxmail.com)
Queensland Brain Institute
The University of Queensland
Brisbane, QLD 4072, Australia

MRR (m.robinson11@uq.edu.au)
Queensland Brain Institute
The University of Queensland
Brisbane, QLD 4072, Australia

Abstract

We apply the statistical framework for genome-wide association studies (GWAS) to eigenvector decomposition (EigenGWAS), which is commonly used in population genetics to characterise the structure of genetic data. The approach does not require discrete sub-populations and thus it can be utilized in any genetic data where the underlying population structure is unknown, or where the interest is assessing divergence along a gradient. Through theory and simulation study we show that our approach can identify regions under selection along gradients of ancestry. In real data, we confirm this by demonstrating *LCT* to be under selection between HapMap CEU-TSI cohorts, and validated this selection signal across European countries in the POPRES samples. *HERC2* was also found to be differentiated between both the CEU-TSI cohort and within the POPRES sample, reflecting the likely anthropological differences in skin and hair colour between northern and southern European populations. Controlling for population stratification is of great importance in any quantitative genetic study and our approach also provides a simple, fast, and accurate way of predicting principal components in independent samples. With ever increasing sample sizes across many fields, this approach is likely to be greatly utilized to gain individual-level eigenvectors avoiding the computational challenges associated with conducting singular value decomposition in large datasets. We have developed freely available software to facilitate the application of the methods.

Introduction

In population genetics, eigenvectors have been routinely used to quantify genetic differentiation across populations and to infer demographic history (Cavalli-Sforza *et al.*, 1996; Novembre *et al.*, 2008; Reich *et al.*, 2009). More recently, eigenvectors are commonly used as covariates in genome-wide association studies (GWAS) to adjust for population stratification (Price *et al.*, 2006). Eigenvectors are usually estimated for each individual (individual-level eigenvectors, involving the inversion of a $N \times N$ matrix, where N is sample size). Theoretical studies have suggested that individual-level primary eigenvectors are measures of population differentiation reflecting F_{st} among subpopulations (Patterson *et al.*, 2006; McVean, 2009; Bryc *et al.*, 2013) and can be interpreted as the divergence of individuals from their most recent common ancestor. Eigenvectors can also be estimated for each SNP (SNP-level eigenvectors, which involve inversion of a $M \times M$ matrix, M is the number of SNPs) and these SNP-level eigenvectors can be interpreted as F_{st} metrics of each SNP (Weir, 1996). SNP-level eigenvectors from a reference population are useful for revealing the population structure of independent samples (Zhu *et al.*, 2008) as they can be used to project, or predict, the eigenvector values of individuals. However, due to high-dimensional nature of GWAS data (commonly expressed as $M \gg N$), direct estimation of SNP-level eigenvectors is nearly impossible when using millions of single nucleotide polymorphisms (SNPs).

Singular value decomposition (SVD) enables SNP-level eigenvalues to be obtained in a computationally efficient manner for any set of genotype data (Chen *et al.*, 2013), however, it is not possible to determine the SNPs that contribute most to the leading eigenvector, or to test whether specific SNPs are differentiated along the genetic gradient described by the eigenvector. Here, we propose an alternative simple, fast approach for the estimation of SNP-level eigenvectors. By using individual-level eigenvectors as phenotypes in a linear regression, we demonstrate that the regression coefficients generated by single-SNP regression are equivalent to SVD SNP effects as proposed by Chen et al (Chen *et al.*, 2013). As the single-SNP regression resembles the popular single-marker GWAS method, as implemented in PLINK (Purcell *et al.*, 2007), we call this method EigenGWAS. We show that the EigenGWAS framework represents an alternative way for identifying regions under selection along gradients of ancestry.

Results

Properties of the estimating SNP effects for eigenvectors

We applied EigenGWAS to the HapMap cohort, a known structured population. Eigenvectors were estimated via principal component analysis based on the $\boldsymbol{A}$ matrix using all 919,133 SNPs. We conducted EigenGWAS for HapMap, using E_k, the k^{th} eigenvector, as the phenotype and investigated the performance of EigenGWAS from E_1 to E_{10}. From E_1 to E_{10}, we found 546,716 significant signals (231,677 quasi-independent signals after clumping) on E_1 and gradually reduced to 236 (163 after clumping) selection signals on E_{10} (**Fig. 1**). The large number of genome-wide significant loci are likely because HapMap3 was comprised of samples from different ethnicities, and these loci can be interpreted as ancestry informative marker (AIM). For each E_k, its associated eigenvalue was highly correlated with the λ_{GC}, the genomic inflation factor that is commonly used in adjusting population stratification for GWAS (Devlin and Roeder, 1999), resulted from its EigenGWAS. The top five eigenvalues associated to HapMap samples were 100.14, 47.66, 7.168, 5.92, and 4.40, and the corresponding λ_{GC} of EigenGWAS were 103.72, 44.69, 6.47, 5.17, and 3.96, respectively (**Table 1**). The large eigenvalues observed were consistent with previous theory that the magnitude of eigenvalues indicating structured population (Patterson *et al.*, 2006). The connection between λ_{GC} and eigenvalues, provides a straightforward interpretation: a large λ_{GC} indicates underlying population structure (Devlin and Roeder, 1999). Therefore, correction for λ_{GC} will filter out signals due to population stratification, allowing loci under selection to be identified. These observations agreed well with our theory (see Methods & Materials).

We demonstrate theoretically that for EigenGWAS, the estimated SNP effects using single-marker GWAS are equivalent to the estimates from BLUP, and the correlation between the estimates from these two methods was very high (greater than 0.98 on average) (**Fig. 2**), even in HapMap samples that consist of a mix of ethnicities where the $\boldsymbol{A}$ matrix is non-zero for off-diagonal elements (**Supplementary Fig. 1**). This confirms that our EigenGWAS approach provides an accurate representation of the SNP effects on eigenvalues.

We also conducted EigenGWAS on the POPRES samples, from which we selected 2,466 European samples. On E_1, there were 10,885 (3,004 quasi-independent signals after

clumping) genome-wide significant signals, and reduced to 1,639 (90 after clumping) on E_{10} (**Table 1**). As in the HapMap sample, we observed a concordance between eigenvalues and λ_{GC} in POPRES. The top five eigenvalues were 5.104, 2.207, 2.157, 2.077, and 1.971, with their associated EigenGWAS λ_{GC} were 5.005, 1.929, 1.910, 1.464, and 1.866, respectively (**Table 1**), indicating population structure. The genetic relationship matrix (GRM) estimated from the POPRES data resembled a diagonal matrix, which had off-diagonal elements close to zero, suggesting that POPRES is a more homogenous samples as compared to HapMap (**Supplementary Fig. 1**). Correlations between the estimates from EigenGWAS and BLUP were high, with an average of greater than 0.999 from E_1 to E_{10} (**Supplementary Fig. 2**), close to one as expected.

The chi-square statistics of the estimated SNP effects on eigenvectors from EigenGWAS were correlated with F_{st} for each SNP, consistent with previous established relationship between eigenvectors and F_{st} (Patterson *et al.*, 2006; McVean, 2009). Using naïve threshold of $E_k > 0$, 2,466 POPRES samples were divided into nearly two even groups, which would be served as two subgroups in calculating F_{st}. $E_1 > 0$ split the POPRES samples into North and South Europe; samples from UK, Ireland, Germany, Austria, and Australia were in one group, and samples from Italy, Spain, and Portugal were in the other group; samples from Switzerland and France were nearly evenly split into two groups. F_{st} for each SNP was consequently calculated based on these two groups. For every eigenvector until E_{10}, we observed strong correlations between F_{st} and the chi-square test statistics for EigenGWAS signals (**Fig. 3**), and the averaged correlation was 0.925 (S.D., 0.067). For example, the correlation was 0.89 (p-value<1e-16) between chi-square test statistics and F_{st} for E_1 in POPRES (**Supplementary Table 1**). This correlation is consistent with our theory, where F_{st} has a strong linear relationship with its EigenGWAS chi-square test statistic.

We also validated our results in the simulation scheme I, in which there was neither selection nor population stratification. Given 2,000 simulated samples, each of which had 500,000 unlinked SNPs, the EigenGWAS showed few GWAS signals (2 genome-wide significant signals on E_1, (**Supplementary Fig. 4**). After splitting the samples into 2 groups depending on $E_i > 0$, the correlation between chi-square test statistics and F_{st} is about 0.67 from E_1 to E_{10} (**Supplementary Fig. 5**). As expected, λ_{GC} ranged from around 1.124 to 1.130, with a mean of 1.124 for EigenGWAS on the top 10 eigenvectors, indicating little population

stratification for the simulated data. Furthermore, we also validated the theory in the simulation scheme II, in which there was population stratification. We wanted to know whether the adjustment of the test statistic with the greatest eigenvalue could render the distribution of the test statistics immunes of population stratification. Given various sample sizes for two subdivisions, after the adjustment for the test statistic with the largest eigenvalue, the test statistic followed the null distribution, which was a chi-square distribution of 1 degree of freedom (**Supplementary Fig. 6**), indicating a well control of population stratification after correction. The statistical power of EigenGWAS was also evaluated. As demonstrated, the power of EigenGWAS in detecting a locus under selection was determined by the ratio between the specific F_{st} of a locus and the averaged population stratification in the sample (**Supplementary Fig. 7**).

Using EigenGWAS to identify loci under selection in structured populations

We propose EigenGWAS as a method of finding loci differentiated among populations, or across a gradiant of ancestry. Intuitively, every EigenGWAS hit is an AIM, which differ in allele frequency along an eigenvector due to genetic drift or selection. A locus under selection should be more differed across populations than genetic drift can bring out. Thus, correction for λ_{GC}, controls for background population structure, providing a test of whether an AIM shows greater allelic differentiation than expected under the process of genetic drift.

We pooled together CEU (112 individuals) and TSI (88 individuals), which represent Northwestern and Southern European populations in HapMap. EigenGWAS was conducted on E_1, which partitioned CEU and TSI into two groups accurately using $E_1 > 0$ as threshold (**Supplementary Fig. 8**). We corrected for λ_{GC}, which was 1.723, for CEU&TSI. Adjustment for λ_{GC} significantly reduced population stratification (**Supplementary Fig. 9**), and was consequently possible to filter out the baseline difference between these two cohorts. After correction, we found evidence of selection at the lactose persistence locus, *LCT* (*p*-value=1.21e-20). Due to hitchhiking effect, the region near *LCT* also showed divergent allele frequencies. For example, the *DARS* gene, 0.15M away from *LCT*, was also significantly associated with E_1 (*p*-values=1.51e-23). *HERC2* was slightly below genome-wide significance level (*p*-value=8.22e-08), indicating that anthropological difference reflected geographic locations of two cohorts but not under selection as strong as *LCT*.

We then conducted EigenGWAS in the POPRES sample by treating E_1 as a quantitative trait, and calculated the approximate F_{st} for each SNP given two groups split by the threshold of $E_1 > 0$ (**Supplementary Fig. 10**). Given 643,995 SNPs, the genome-wide threshold was *p*-value < 7.76e-08 for the significance level of $\alpha = 0.05$. $\lambda_{GC} = 5.00$, which indicated substantial population stratification as expected for POPRES. Correcting for λ_{GC} systematically reduced the EigenGWAS χ^2 test statistics (**Supplementary Fig. 11**), and we replicated the significance of *LCT* (*p*-value=1.23e-22) and *DARS* (*p*-value=8.99e-22) (**Table 2**), suggesting selection at these regions. *HERC2* was also replicated with *p*-value 8.15e-09, and with F_{st} of 0.041.

Prediction accuracy for projected eigenvector

We investigated three aspects of EigenGWAS prediction: 1) the number of loci needed to achieve high accuracy for the projected eigenvectors; 2) the required sample size of the training set; 3) the importance of matching the population structure between the training and the test sets.

Using the POPRES samples, we split 5% (125 individuals), 10% (250 individuals), 20% (500 individuals), 30% (750 individuals), 40% (1000 individuals), and 50% (1250 individuals) of the sample as the training set, and used the remainder of the samples as the test set. Eigenvectors were estimated using all markers in each training set. As predicted by our theory (Eq 7), the prediction accuracy of the projected eigenvector was consistent with $R^2 = \frac{1}{1+\frac{Ne}{M}}$ in which $N_e = 1{,}000$ for E_1 empirically. If only 100 and 1,000 random SNPs were sampled as predictors, the expected maximal $R^2 = 0.091$ and 0.5, respectively and accuracy reached almost 1 if more than 100,000 SNPs were sampled. In agreement with our theory (**Fig. 6**), if the number of predictors were too small the prediction accuracy was poor, with prediction accuracy increasing with the addition of more markers for E_1. When the sample size of the discovery was 1,000 or above, maximal prediction accuracy was achieved, as predicted in our theory. Therefore, a discovery with a sample size greater than 1,000 should be sufficient to predict the first eigenvector of an independent set, provided that population structure is the same across the discovery and prediction samples (**Fig. 6**). In contrast, the prediction accuracy for prediction eigenvectors decreased (**Fig. 6**) quickly for eigenvectors other than E_1. For example, the prediction accuracy for E_2 was below $R^2 < 0.2$ and $R^2 < 0.15$ for E_3. For $E_4 \sim E_{10}$, the prediction accuracy dropped down to nearly zero. This is

consistent with the top 2~3 eigenvectors explaining the majority of variation (McVean, 2009), if the training and the test sets had their population structure matched.

If EigenGWAS SNPs of low *p*-value were likely to be AIMs, we would hypothesise that AIM markers would be more efficient in giving high accuracy for the predicted eigenvectors (**Fig. 6**). For E_1, the prediction accuracy reached 1 more quickly by using markers selected by *p*-value thresholds. The prediction accuracy for projected E_2 was dependent upon the threshold. For projected E_2 given a 50:50 split of POPRES sample, applying the threshold of *p*-value < 1e-6 (927 SNPs), $R^2 = 0.136$, as high as using all markers. For other projected eigenvectors, the pattern of accuracy did not change much after applying *p*-value thresholds because in general, the prediction accuracy was low. This indicated that eigenvectors other than the first two eigenvectors capture little replicable population structure in POPRES.

In practice, the training and the test set may not match perfectly on population structure, and this will likely lead to a reduction in prediction accuracy. To demonstrate this, we split the POPRES samples into two sets: pooling Swiss (991 samples) and French (96 samples) samples into one group (SF), and the rest of the samples into the other group (NSF). We used SF as the training and the NSF as the testing. As SF was almost an average of North European and South European gene flow, making a less stratified population, its EigenGWAS effects would be consequently small and less "heritable". When using all SNPs effects estimated from SF set, the observed prediction accuracy for NSF set was $R^2 = 0.33$ and 0.005 for E_1 and E_2, respectively. These results indicate that a matched training and test set is important for prediction accuracy of the projected eigenvectors.

Ancestry information may still be elucidated well even if the training set and the test set do not match well in their population structure. Using HapMap3 as the training set, we also tried to infer the ancestry of the Puerto Rican cohort (PUR, 105 individuals) and Pakistani cohorts (PJL, 95 individuals) from 1000 Genomes project (The 1000 Genomes Project Consortium, 2012). In chromosome 1, 74,500 common SNs were found between HapMap3 and 1000 Genomes project. As illustrated, using only 74,500 common markers between HapMap3 and 1000 Genome projects SNPs on chromosome 1, it projected Eigenvectors accurately revealed the demographic history of Puerto Rican cohort, an admixture of African and European gene flows, and Pakistan cohort, an admixture of Asian and European gene flows (**Fig. 7**).

As a negative control, we replicated the prediction study for simulated data used in the previous section. The simulated data was split to two equal sample size. As there was no population structure in the simulated data, the prediction accuracy was poor, $R^2 < 0.01$ from E_1 to E_{10}. This demonstrates that prediction can be used to validate whether population structure exists within a genotype sample.

We concluded that to achieve high prediction accuracy of projected eigenvectors for independent samples, there are several conditions to be met: 1) the training set should harbour sufficient population stratification; 2) the sample size of the training should be sufficiently large; 3) the test sets should be as concordant as possible in its population structure; 4) when there is no real population structure, the prediction accuracy is very low close to zero; 5) depending on the population, high prediction was largely achievable for the projected E_1.

Discussion

Eigenvectors have been routinely employed in population genetics, and various approaches have been proposed to offer interpretation and efficient algorithms (Patterson *et al.*, 2006; Rokhlin *et al.*, 2009; McVean, 2009; Chen *et al.*, 2013; Galinsky *et al.*, 2015). In this study, we created a GWAS framework for studying and validating population structure, and offer an interpretation of eigenvectors within this framework. The EigenGWAS framework (least square) identifies ancestry informative markers and loci under selection across gradients of ancestry.

We integrated SVD, BLUP, and single-marker regression into a unified framework for the estimation of SNP-level eigenvectors. SVD is a special case of BLUP when heritability is of 1 for the trait and the target phenotype is an eigenvector. Furthermore, the BLUP is equivalent to the commonly used GWAS method for estimating SNP effects. As demonstrated, the correlation between BLUP and GWAS is almost 1 for the estimated SNP effects. EigenGWAS offers an alternative way in estimating F_{st} that can replace conventional F_{st} when population labels are unknown, populations are admixed, or differentiation occurs

278 across a gradient. As demonstrated for CEU&TSI samples, EigenGWAS brings out nearly
279 identical estimation of F_{st} compared with conventional estimation.
280
281 Different from conventional GWAS, which requires conventional phenotypes, the proposed
282 EigenGWAS provides a novel method for finding loci under selection based on eigenvectors,
283 which are generated from the genotype data itself. An EigenGWAS hit may reflect the
284 consequence of process and thus additional evidence is needed to differentiate selection from
285 drift. *LCT* is a known locus under selection, which differs in its allele frequency as indicated
286 by F_{st} statistic between Northern and Southern Europeans (Bersaglieri *et al.*, 2004). We
287 replicated the significance of *LCT* in CEU&TSI samples and POPRES European samples.
288 *DARS* has been found in association with hypomyelination with brainstem and spinal cord
289 involvement and leg spasticity (Taft *et al.*, 2013). In addition, we also found *HERC2* locus
290 independently, which may indicate the existence of anthropological difference in certain
291 characters, such as hair, skin, or eyes color across European nations (Voight *et al.*, 2006;
292 Visser *et al.*, 2012).
293
294 Although by definition selection and genetic drift are different biological processes, both lead
295 to allele frequency differentiation across populations and often difficult to tear them apart. In
296 this study, with and without adjustment for λ_{GC} from EigenGWAS offers a straightforward
297 way to filter out population stratification. For example, with adjustment for λ_{GC}, *LCT* and
298 *DARS* were still significant in both EigenGWAS, while *HERC2* was only significant in
299 POPRES. If adjustment for λ_{GC} removed the average genetic drift since the most recent
300 common ancestor for the whole sample, it might indicate that *HERC2* reflected the
301 anthropological difference between subsamples but not under selection as strong as that for
302 *LCT*. Nevertheless, *LCT* was differentiated due to selection that was on top of genetic drift,
303 and for *DARS*, it might be significant due to hitchhiking effect. So, *LCT*, *DARS*, and *HERC2*
304 were significant in EigenGWAS for different mechanisms.
305
306 In EigenGWAS application, it provides a clear scenario that λ_{GC} is necessary if genetic
307 drift/population stratification should be filtered out. It has been debated whether correction
308 for λ_{GC} is necessary for GWAS (Devlin and Risch, 1995; Yang, Weedon, *et al.*, 2011). If the
309 inflation is due to population stratification, as initially λ_{GC} introduced, it seems necessary to
310 control for it. In contrast, if it is due to polygenic genetic architecture, then correction for λ_{GC}

will be a overkilling for GWAS signals. Interestingly, Patterson et al (Patterson *et al.*, 2006) found that the top eigenvalues reflect population stratification, and in our study we found λ_{GC} from EigenGWAS was numerically so similar to its corresponding eigenvalues. It in another aspect indicates λ_{GC} captures population stratification. So, in concept and implementation, the correction for λ_{GC} is technically reasonable. Of note, Galinsky et al also proposed a similar procedure to filter out population stratification in a study similar to ours (Galinsky *et al.*, 2015), but we believe our framework is much easier to understand and implement in practice.

Once we have EigenGWAS SNP effects estimated, it is straightforward to project those effects onto an independent sample. The prediction of population structure was to that of recent studies (Chen *et al.*, 2013). We found that the prediction accuracy for the top eigenvector could be as high as almost 1. Given a training set of about 1,000 samples, the prediction accuracy could be very high if there were a reasonable number of common markers in the order of 100,000. This number, which needs to be available in both reference set and the target set, is achievable. Further investigation may be needed to check whether this number of markers is related to effective number or markers after correction for linkage disequilibrium for GWAS data. When the population structure of the test sample resembles the training sample, high accuracy will be achieved for the leading projected eigenvectors. Therefore, this approach is likely to be extremely beneficial for extremely large samples, such as UK Biobank samples and 23andMe, both of which have more than half million samples where direct eigenvector analysis may be infeasible. Our results suggest that sampling about 1,000 individuals from the whole sample as the training set and subsequently project EigenGWAS SNP effects to the reminding samples will be sufficient to reach a reasonable high resolution of the population structure.

Many improvements to the inference of ancestry using projected eigenvectors have been suggested (Chen *et al.*, 2013). As the concordance of population structure between the training and test sets is often unknown (population structure, upon from genetic or social-cultural perspectives, its definition can be difficult or controversial), improvement of the inference of ancestry may or may not be achieved dependent upon the scale of the precision required for a sample. However, for classification of samples at ethnicity level, projected eigenvectors are likely to have high accuracy, as demonstrated in the Puerto Rican cohort and

the Pakistani cohort. Therefore, when identifying ethnic outliers, using projected eigenvectors from HapMap is likely to be sufficient in practice.

Eigenvector analysis of GWAS data is an important well utilized data technique, and here we show that its interpretation depends on many factors, such as proportion of different subpopulations, and F_{st} between subpopulations. Our EigenGWAS approach provides intuitive interpretation of population structure, enabling ancestry informative markers (AIM) to be identified, and potentially loci under selection to be identified. To facilitate the use of projected eigenvectors, we provide estimated SNP effects from HapMap samples and POPRES and software that can largely reduce the logistics involved in conventional way in generating eigenvectors, such as reference allele match, and strand flips.

Methods and Materials

HapMap3 samples. HapMap3 samples were collected globally to represent genetic diversity of human population (Altshuler *et al.*, 2010). HapMap3 contains representative samples from many continents: CEU and TSI represent population from north and south Europe, CHB and JPT from East Asia, and CHD Chinese collected in Denver, Colorado. Loci with palindrome alleles (A/T alleles, or G/C alleles) were excluded, and 919,133 HapMap3 SNPs were used for the analysis.

1000 Genomes project. 1000 Genomes project samples were used as a prediction set for projecting eigenvectors (The 1000 Genomes Project Consortium, 2012). We selected the Puerto Rico cohort (PUR, 105 samples) and the Pakistan cohort (Punjabi from Lahore, Pakistan, 95 samples) for analysis.

POPRES samples. POPRES (Nelson *et al.*, 2008) is a reference population for over 6,000 samples from Asian, African, and European nations. In this study, we selected 2,466 European descendants. The POPRES genotype sample was imputed to a 1000 Genomes reference panel (The 1000 Genomes Project Consortium, 2012). Imputation for the POPRES was performed in two stages. First, the target data was haplotyped using HAPI-UR (Williams *et al.*, 2012). Second, Impute2 was used to impute the haplotypes to the 1000 genomes reference panel (Howie *et al.*, 2011). We then selected SNPs which were present across all datasets at an imputation information score of >0.8. A full imputation procedure is described

at https://github.com/CNSGenomics/impute-pipe. After quality control and removing loci with palindromic alleles (A/T alleles, or G/C alleles) 643,995 SNPs for POPRES remained. In addition, we also conducted the analysis using non-imputed 234,127 common markers between POPRES and HapMap3. As the results were between these two datasets were very similar, this report focused on the results from 643,995 SNPs, which were more informative.

Simulation scheme I: null model without population structure. 2,000 unrelated samples with 500,000 biallelic markers, which were in linkage equilibrium to each other, were simulated. The minor allele frequencies ranged from 0.01~0.5, and Hardy-Weinberg equilibrium was assumed for each locus. All individuals were simulated from a homogeneous population, with no population stratification. In order to calculate F_{st} at each locus, we divided the sample into sub-populations based upon eigenvectors that were estimated from a genetic relationship matrix calculated using all 500,000 markers (see below).

Simulation scheme II: null model with population structure. In general, this simulation scheme was followed Price et al (Price *et al.*, 2006). 2,000 unrelated samples with 10,000 biallelic markers, which were in linkage equilibrium to each other, were generated. For each marker, its ancestral allele frequency was sampled from a uniform distribution between 0.05 to 0.95, and its frequency in a subpopulation was sampled from Beta distribution with parameters $p\frac{1-F_{st}}{F_{st}}$ and $(1-p)\frac{1-F_{st}}{F_{st}}$. The Beta distribution had mean of p and sampling variance of $p(1-p)F_{st}$. Once the allele frequency for a subpopulation over a locus was determined as p_s, individuals were generated from a binomial distribution $Binomil(2, p_s)$. It agreed with the quantity that measures the genetic distance between a pair of subpopulations (Cavalli-Sforza *et al.*, 1996).

Calculating individual-level eigenvectors

We assume that there is a reference sample consisting of N unrelated individuals and M markers. $X_i = (x_{i1}, x_{i2}, \ldots, x_{iM})^T$, is a vector of the i^{th} individual's genotypes along M loci, with x the number of the reference alleles. An $N \times N$ genetic relatedness (correlation) matrix $\boldsymbol{A}$ (matrix in bold font) for each pair of individuals is defined as $A_{ij} = \frac{1}{M}\Sigma_{l=1}^{M}\frac{(x_{il}-2f_l)(x_{jl}-2f_l)}{2f_l(1-f_l)}$, in which f_l is the frequency of the reference allele. The principal component analysis (PCA)

is then implemented on the A matrix (Price *et al.*, 2006), generating $\mathbb{E}$, which is an $N \times K$ ($K \leq N$) matrix, in which E_k is the eigenvector corresponding to the k^{th} largest eigenvector.

Unified framework for BLUP, SVD, and EigenGWAS

Theoretically, PCA can also be implemented on a $M \times M$ matrix, but this is often infeasible because the $M \times M$ matrix is very large. However, for individual i, eigenvector k can also be written as:

$$E_{k,i} = \beta_k \boldsymbol{X}_i^T \qquad \textbf{(Equation 1)}$$

in which β_k is a $M \times 1$ SNP-level vector of the SNP effects on E_k, and x_i is the genotype of the i^{th} individual across M loci. In the text below, we denote individual-level eigenvector as eigenvector ($N \times 1$ vector), and SNP-level eigenvector ($M \times 1$) as SNP effects.

We review three possible methods to estimate β given eigenvectors. The first method is best linear prediction (BLUP), which is commonly used in animal breeding and recently has been introduced to human genetics for prediction (Henderson, 1975; Goddard *et al.*, 2009). The second method is to convert an individual-level eigenvector to SNP-level eigenvector using SVD, as proposed by Chen et al (Chen *et al.*, 2013). The third method is the approach outlined here, EigenGWAS, which is a single-marker regression, as commonly used in GWAS analysis.

Method 1 and 2: BLUP and SVD

For a quantitative trait, $y = \mu + \beta \boldsymbol{X} + e$, in which y is the phenotype, μ is the grand mean, β is the vector for additive effects, X is the genotype matrix, and e is the residual. Without loss of generality, the BLUP equation can be expressed as:

$$\hat{\beta} = \widetilde{\boldsymbol{X}}^T \boldsymbol{V}^{-1} y \qquad \textbf{(Equation 2)}$$

in which $\hat{\beta}$ is the estimates of the SNP effects, $\widetilde{\boldsymbol{X}}$ is the standardized genotype matrix, $\boldsymbol{V}$ is the variance covariance with $\boldsymbol{V} = {\sigma_A}^2 \boldsymbol{A} + \left(\sigma_y^2 - {\sigma_A}^2\right)\boldsymbol{I}$, and y is the trait of interest (Henderson, 1975). Replacing y with individual-level eigenvector (E_k), Eq 2 can be written as

$$\hat{\beta}_k = \widetilde{\boldsymbol{X}}^T \boldsymbol{A}^{-1} E_k \qquad \textbf{(Equation 3)}$$

in which β_k is the BLUP estimate of the SNP effects, E_k is the k^{th} eigenvector estimated from the reference sample., The $\boldsymbol{V}$ matrix can be replaced with $\boldsymbol{A}$ because the eigenvector has no residual error (i.e. h^2=1). This method has also been proposed as an equivalent computing algorithm for genomic predictions (Maier *et al.*, 2015).

In addition, the connection between PCA and SVD can be established through the transformation between the $N \times N$ matrix to the $M \times M$ matrix (McVean, 2009). Let $\boldsymbol{A} = \boldsymbol{P}\boldsymbol{D}\boldsymbol{P}^{-1}$, in which $\boldsymbol{D}$ is a $N \times N$ diagonal matrix with λ_k, $\boldsymbol{P}$ is $N \times N$ matrix with the eigenvectors. $\boldsymbol{B} = \boldsymbol{X}^T(\boldsymbol{P}\boldsymbol{D}\boldsymbol{P}^{-1})^{-1}\boldsymbol{P} = \boldsymbol{X}^T\boldsymbol{P}\boldsymbol{D}^{-1}$, in which $\boldsymbol{B}$ is $M \times N$ matrix. This is equivalent to the equation used in Chen et al (Chen *et al.*, 2013) where $\boldsymbol{B}^T = \boldsymbol{D}^{-1}(\boldsymbol{X}^T\boldsymbol{P})^T$. Thus, eigenvector transformation can be viewed as a special case of BLUP in which the heritability is 1 (Eq 3). However, under SVD another analysis step is then required to evaluate the significance of the estimated SNP effect. In an EigenGWAS framework an empirical *p-value* is produced when estimating the regression coefficient.

Method 3: estimating SNP effects on eigenvectors with EigenGWAS

Given the realized genetic relationship matrix A, for unrelated homogeneous (i.i.d.) samples, $E(A_{ij}) = 0$ $(i \neq j)$, and consequently $E(\boldsymbol{A}) = \boldsymbol{I}$**, an identity matrix**. Due to sampling variance of the genetic relationship matrix $\boldsymbol{A}$, the off diagonal is a number slightly different from zero even for unrelated samples (Chen, 2014). If we replace the matrix with its mathematical expectation – the identity matrix, Equation 3 can be further reduced to $\beta_k = \widetilde{\boldsymbol{X}}^T E_k$, which is equivalent to single-marker regression $E_k = a + bx + e$, as implemented in PLINK (Purcell *et al.*, 2007). Furthermore, standardization for $\boldsymbol{X}$ is not required because it will not affect *p*-value. Thus, SNP effects can be estimated using the single-marker regression, which is computationally much easier in practice and is implemented in many software packages. Each SNP effect, $\hat{\beta}_{k.m}$, is estimated independently, and the *p*-value of each marker can be estimated, which requires additional steps in BLUP and SVD.

We summarise the properties and their transformation of SVD, BLUP, and EigenGWAS as below:

1) E_k is determined by the $\boldsymbol{A}$ matrix, or in another words, it is determined by the genotypes completely. If we consider each E_k is the trait of interest – a quantitative trait, its heritability is 1.
2) $h^2 = 1$. SVD and BLUP are both computational tool in converting a vector from $N \times N$ matrix to a $M \times M$ matrix. SVD is a special case to BLUP when $h^2 = 1$ for BLUP.

3) $h^2 = 1$ and $E(\boldsymbol{A}) = \boldsymbol{I}$. When these two conditions are set, BLUP is further reduced to single-marker association studies, which is EigenGWAS as suggested in this study.

Recently, in an independent work Galinsky et al (Galinsky *et al.*, 2015) introduced an approximation to find the proper scaling for SNP effects ("SNP weight" in Galinsky's terminology) estimated from SVD, in order to produce accurate *p*-values. In our EigenGWAS framework, *p*-values for individual-level SNP eigenvector are automatically generated. In practice, it is conceptually easier to conduct EigenGWAS on eigenvectors than to conduct BLUP/SVD. Also, if computational speed is of concern, EigenGWAS can be easily parallelized for each chromosome, each region, or even each locus.

Interpretation for EigenGWAS

We can write a linear regression model $E_k = a + \beta x + e$, in which both E_k and x is standardized. Assuming that a sample has two subdivisions, which have sample size n_1 and n_2, $\beta = \frac{2\sqrt{w(1-w)}(p_1-p_2)}{\sqrt{2\bar{p}\bar{q}}}$, and the sampling variance for β is $\sigma_\beta^2 = \frac{\sigma_e^2}{n\sigma_x^2} = \frac{1}{n}$. A chi-square test for β is

$$E(\chi_1^2) = 4nw(1-w)F_{st}^N \quad \textbf{(Equation 4)}$$

in which $F_{st}^N = \frac{(p_1-p_2)^2}{2\bar{p}\bar{q}}$ is Nei's estimator of genetic difference for a biallelic locus (Nei, 1973).

In principal component analysis, the proportion of the variance explained by the largest eigenvalue is equal to F_{st}^W (McVean, 2009), in which $F_{st}^W = \frac{2\sum_{i=1}^{2} w_i[(p_i-\bar{p})^2]}{\bar{p}\bar{q}}$ for a pair of subpopulations as defined in Weir (Weir, 1996). So $\lambda_1 \approx \bar{F}_{st}^W \times n$, in which $\bar{F}_{st}^W$ characterizes the average divergence for a pair of subpopulations. When the test statistic, Eq 4, is adjusted by the largest eigenvalue λ_1, an equivalent technique in GWAS for the correction of population stratification, $E\left(\chi_{1.\lambda_1}^2\right) = \frac{4nw(1-w)F_{st}^N}{\lambda_1} = 4w(1-w)\frac{F_{st}^N}{\bar{F}_{st}^W}$. For a population with a pair of subdivisions $4w(1-w)F_{st}^N = F_{st}^W$. So

$$E\left(\chi_{1.\lambda_1}^2\right) = \frac{F_{st}^W}{\bar{F}_{st}^W} \quad \textbf{(Equation 5)}$$

after the adjustment of the largest eigenvalue, the test statistic immunes of population stratification, at least for a divergent sample.

For a locus under selection, which should have a greater F_{st} than $\bar{F}_{st}$ the background divergence. So the statistical power for detecting whether a locus is under selection is determined by the strength of selection, which can be defined as the ratio between F_{st} of a particular locus and $\bar{F}_{st}$ the average divergent in the sample. It is analogous to consider a chi-square test with non-centrality parameter (NCP), $NCP = \frac{F_{st}^{W}}{\bar{F}_{st}^{W}} - 1$. Otherwise specified, in this study F_{st} is referred to the one defined in Weir (Weir, 1996).

Validation and prediction for population structure

Once β_k is estimated, it is straightforward to get genealogical profile for an independent target sample. In general, it is equivalent to genomic prediction, and the theory for prediction can be applied (Daetwyler *et al.*, 2008; Dudbridge, 2013). The predicted genealogical score can be generated as

$$\tilde{E}_k = \hat{\beta}_{k.m}\boldsymbol{X} \qquad \textbf{(Equation 6)}$$

in which E_k is the predicted k^{th} eigenvector, $\hat{\beta}_{k.m}$ is the estimated SNP effects, and $\boldsymbol{X}$ is the genotype for the target sample. We focus on the correlation between the predicted eigenvectors and the direct eigenvectors, and thus it does not matter whether $\boldsymbol{X}$ or $\widetilde{\boldsymbol{X}}$ is used.

In contrast to conventional prediction studies, which focus on a metric phenotype of interest, prediction of population structure is focussed on a "latent" variable. This latent variable is the genetic structure of population, which is shaped by allele frequency and linkage disequilibrium of markers. Thus, expectations of prediction accuracy differ from what has been established for conventional prediction (Daetwyler *et al.*, 2008; Dudbridge, 2013) $R^2 = h^2\left(\frac{h^2}{h^2+\frac{M}{N}}\right) < h^2 \ll 1$. We therefore assess prediction of accuracy for E_1 across markers, when using different prediction thresholding (Purcell *et al.*, 2009).

Here we proposed an equation for prediction accuracy, especially for E_1

$$R^2 = \frac{\left(h^2+\frac{M}{N_e}\right)^2}{h^2\left(1+2\frac{M}{N_e}\right)+\frac{M}{N_e}\left(1+\frac{M}{N_e}\right)} \approx \frac{1}{1+N_e/M} \qquad \textbf{(Equation 7)}$$

when there is no heritability, the predictor can be simplified to $R^2 = \frac{1}{1+\frac{N_e}{M}}$, meaning that as the number of markers increases prediction accuracy should rapidly reach 1. Here the h^2 is interpreted as the genetic difference in the source population, or real ancestry informative

markers. For a homogeneous population, the genetic difference is large due to genetic drift, and $h^2 \approx 0$.

For this study, the genetic relationship matrix (***A*** matrix), principal component analysis, and BLUP estimation were conducted using GCTA software (Yang, Lee, *et al.*, 2011). Single-marker GWAS was conducted using PLINK (Purcell *et al.*, 2007), or GEAR (https://github.com/gc5k/GEAR/wiki/EigenGWAS; https://github.com/gc5k/GEAR/wiki/ProPC).

Web resource and data availability

GEAR is available at http://cnsgenomics.com/

GCTA is available at http://cnsgenomics.com/

PLINK is available at http://pngu.mgh.harvard.edu/~purcell/plink/index.shtml

1000 Genomes Project: http://www.1000genomes.org/

Acknowledgements

This research was funded by ARC (DE130100614 to SHL), NHMRC (APP1080157 to SHL, APP1084417 and APP1079583 to BB, and APP1050218 to MRR), and GBC was supported by IAP P7/43-BeMGI from the Belgian Science Policy Office Interuniversity Attraction Poles (BELSPO-IAP) program. We thank Peter M. Visscher for discussion, helpful comments, and for proposing the name EigenGWAS. Robert Maier assisted with ggplot, and Alex Holloway helped with Github. We also thank to the Information Technology group, the Queensland Brain Institute. The POPRES dataset were obtained from dbGaP at http://www.ncbi.nlm.nih.gov/gap through accession number phs000145.v4.p2.

Author contributions: GBC, SHL, and BB conceived study. GBC, SHL, BB, and MRR designed the experiment. GBC and SHL developed the theory and methods. BB conducted the quality control for HapMap data, and MRR conducted quality control for POPRES data. GBC performed the analyses of the study. GBC and ZXZ developed GEAR software. GBC, MRR, SHL, and BB wrote the paper.

References

Altshuler DM, Gibbs RA, Peltonen L, Dermitzakis E, Schaffner SF, Yu F, *et al.* (2010). Integrating common and rare genetic variation in diverse human populations. *Nature*

467: 52–8.

Bersaglieri T, Sabeti PC, Patterson N, Vanderploeg T, Schaffner SF, Drake JA, *et al.* (2004). Genetic Signatures of Strong Recent Positive Selection at the Lactase Gene. *Am J Hum Genet* **74**: 1111–1120.

Bryc K, Bryc W, Silverstein JW (2013). Separation of the largest eigenvalues in eigenanalysis of genotype data from discrete subpopulations. *Theor Popul Biol* **89**: 34–43.

Cavalli-Sforza LL, Menozzi P, Piazza A (1996). *The History and Geography of Human Genes*. Princeton University Press.

Chen G-B (2014). Estimating heritability of complex traits from genome-wide association studies using IBS-based Haseman-Elston regression. *Front Genet* **5**: 107.

Chen C-Y, Pollack S, Hunter DJ, Hirschhorn JN, Kraft P, Price AL (2013). Improved ancestry inference using weights from external reference panels. *Bioinformatics* **29**: 1399–406.

Daetwyler HD, Villanueva B, Woolliams J a (2008). Accuracy of predicting the genetic risk of disease using a genome-wide approach. *PLoS One* **3**: e3395.

Devlin B, Risch N (1995). A comparison of linkage disequilibrium measures for fine-scale mapping. *Genomics* **29**: 311–22.

Devlin B, Roeder K (1999). Genomic control for association studies. *Biometrics* **55**: 997–1004.

Dudbridge F (2013). Power and predictive accuracy of polygenic risk scores. *PLOS Genet* **9**: e1003348.

Galinsky KJ, Bhatia G, Loh P, Georgiev S, Mukherjee S, Nick J (2015). Fast principal components analysis reveals independent evolution of ADH1B gene in Europe and East Asia. *bioRxiv*: http://dx.doi.org/10.1101/018143.

Goddard ME, Wray NR, Verbyla K, Visscher PM (2009). Estimating Effects and Making Predictions from Genome-Wide Marker Data. *Stat Sci* **24**: 517–529.

Henderson CR (1975). Best Linear Unbiased Estimation and Prediction under a Selection Model. *Biometrics* **31**: 423–447.

Howie B, Marchini J, Stephens M, Chakravarti A (2011). Genotype Imputation with Thousands of Genomes. *G3* **1**: 457–470.

Maier R, Moser G, Chen G, Ripke S, Group CW, Consortium PG, *et al.* (2015). Joint Analysis of Psychiatric Disorders Increases Accuracy of Risk Prediction for Schizophrenia, Bipolar Disorder, and Major Depressive Disorder. *Am J Hum Genet* **96**: 283–294.

McVean G (2009). A genealogical interpretation of principal components analysis. *PLOS Genet* **5**: e1000686.

Nei M (1973). Analysis of gene diversity in subdivided populations. *Proc Natl Acad Sci U S A* **70**: 3321–3.

Nelson MR, Bryc K, King KS, Indap A, Boyko AR, Novembre J, *et al.* (2008). The Population Reference Sample, POPRES: A Resource for Population, Disease, and Pharmacological Genetics Research. *Am J Hum Genet* **83**: 347–358.

Novembre J, Johnson T, Bryc K, Kutalik Z, Boyko AR, Auton A, *et al.* (2008). Genes mirror geography within Europe. *Nature* **456**: 98–101.

Patterson N, Price AL, Reich D (2006). Population structure and eigenanalysis. *PLOS Genet* **2**: e190.

Price AL, Patterson NJ, Plenge RM, Weinblatt ME, Shadick N a, Reich D (2006). Principal components analysis corrects for stratification in genome-wide association studies. *Nat Genet* **38**: 904–9.

Purcell S, Neale B, Todd-Brown K, Thomas L, Ferreira M a R, Bender D, *et al.* (2007). PLINK: a tool set for whole-genome association and population-based linkage analyses. *Am J Hum Genet* **81**: 559–75.

Purcell SM, Wray NR, Stone JL, Visscher PM, O'Donovan MC, Sullivan PF, *et al.* (2009). Common polygenic variation contributes to risk of schizophrenia and bipolar disorder. *Nature* **460**: 748–752.

Reich D, Thangaraj K, Patterson N, Price AL, Singh L (2009). Reconstructing Indian population history. *Nature* **461**: 489–94.

Rokhlin V, Szlam A, Tygert M (2009). A randomized algorithm for principal component analysis. *SIAM J Matrix Anal Appl* **31**: 1100–1124.

Taft RJ, Vanderver A, Leventer RJ, Damiani S a, Simons C, Grimmond SM, *et al.* (2013). Mutations in DARS cause hypomyelination with brain stem and spinal cord involvement and leg spasticity. *Am J Hum Genet* **92**: 774–80.

The 1000 Genomes Project Consortium (2012). An integrated map of genetic variation from 1,092 human genomes. *Nature* **491**: 56–65.

Visser M, Kayser M, Palstra R-J (2012). HERC2 rs12913832 modulates human pigmentation by attenuating chromatin-loop formation between a long-range enhancer and the OCA2 promoter. *Genome Res* **22**: 446–55.

Voight BF, Kudaravalli S, Wen X, Pritchard JK (2006). A map of recent positive selection in the human genome. *PLOS Biol* **4**: e72.

Weir BS (1996). *Genetic data analysis*, 2nd edn. Sinauer Associates, Inc.: Sunderland, MA, USA.

638 Williams AL, Patterson N, Glessner J, Hakonarson H, Reich D (2012). Phasing of many
639 thousands of genotyped samples. *Am J Hum Genet* **91**: 238–251.

640 Yang J, Lee SH, Goddard ME, Visscher PM (2011). GCTA: a tool for genome-wide complex
641 trait analysis. *Am J Hum Genet* **88**: 76–82.

642 Yang J, Weedon MN, Purcell S, Lettre G, Estrada K, Willer CJ, *et al.* (2011). Genomic
643 inflation factors under polygenic inheritance. *Eur J Hum Genet* **19**: 807–12.

644 Zhu X, Li S, Cooper RS, Elston RC (2008). A Unified Association Analysis Approach for
645 Family and Unrelated Samples Correcting for Stratification. *Am J Hum Genet* **82**: 352–
646 365.

647

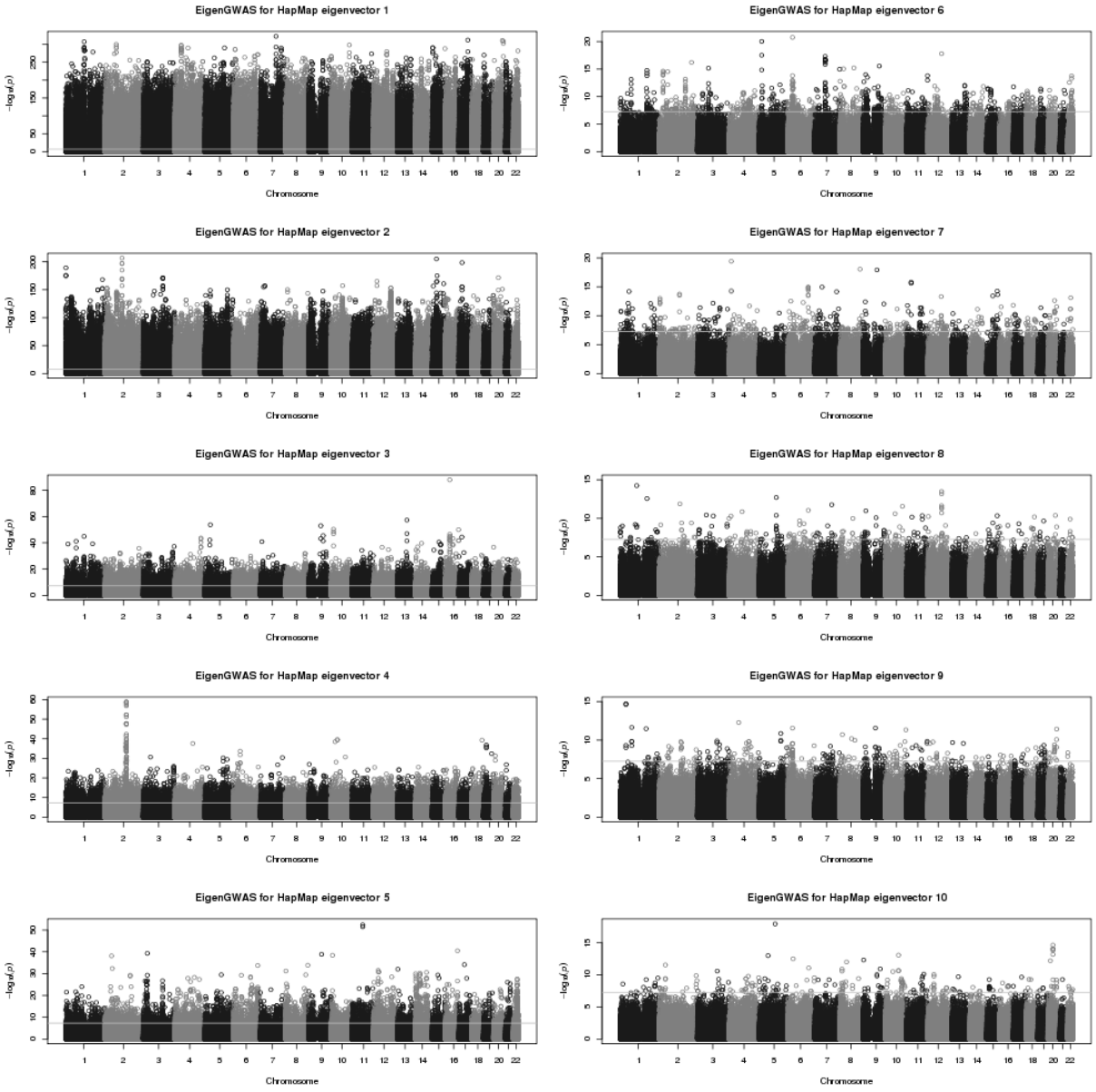

Figure 1 Manhattan plots for EigenGWAS for top 10 eigenvectors for HapMap. Using E_i as the phenotype, the single-marker association was conducted for nearly 919,133 markers. The left panel illustrates from $E_1 \sim E_5$; the right panel from $E_6 \sim E_{10}$. The horizontal lines indicate genome-wide significant after Bonferroni correction.

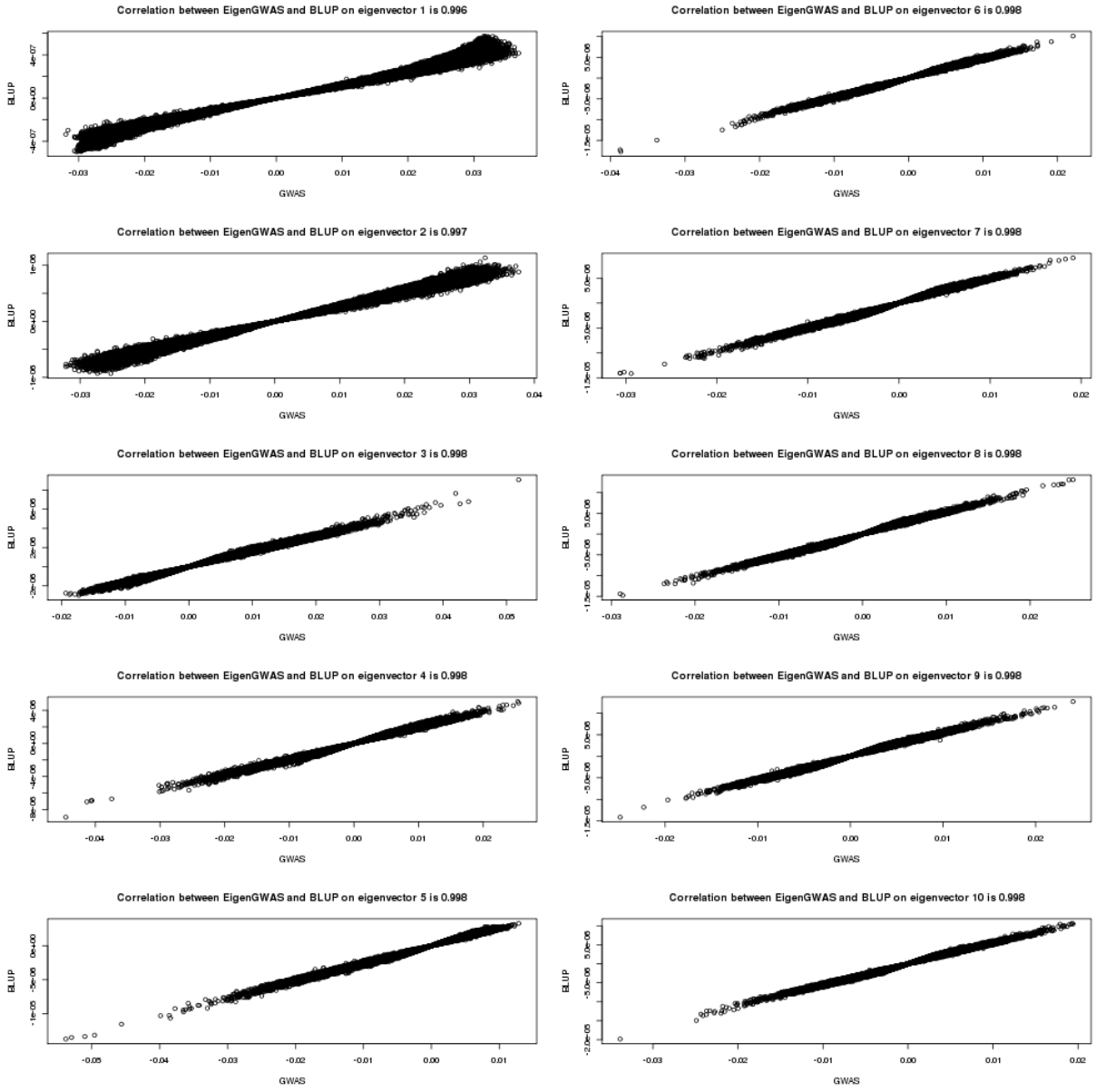

654

655 **Figure 2** Correlation for the SNP effects estimated using EigenGWAS and BLUP for
656 HapMap3. The x-axis represents EigenGWAS estimation for SNP effects, and the y-axis
657 represents BLUP estimation for SNP effects. The left panel illustrates from $E_1 \sim E_5$; the right
658 panel from $E_6 \sim E_{10}$. As illustrated, the correlation is nearly 1.

659

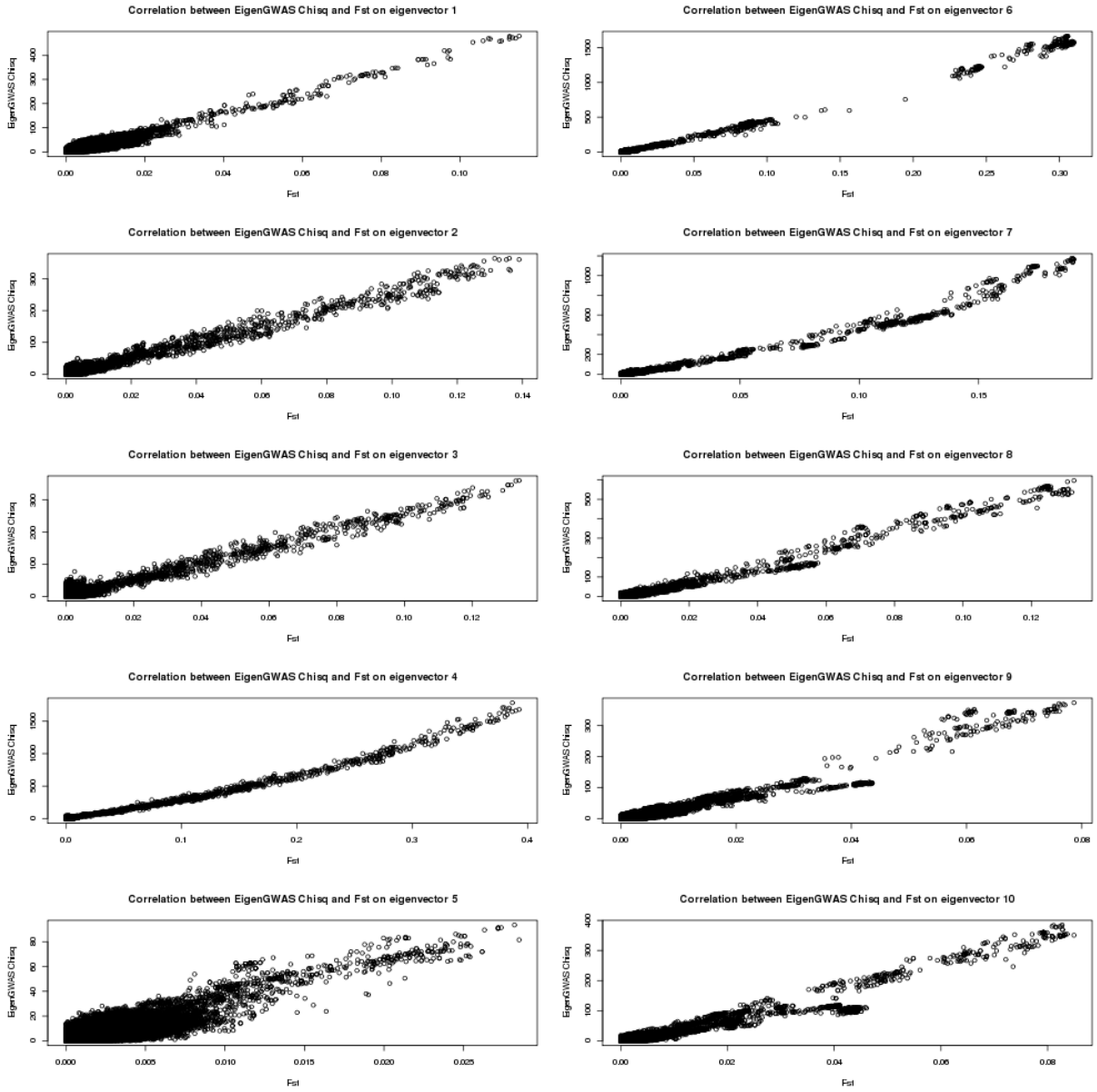

Figure 3 The correlation between F_{st} and χ_1^2 for EigenGWAS SNP effects for POPRES. For each eigenvector, upon $E_i > 0$ or $E_i \leq 0$, the samples were POPRES samples were split into two groups, upon which F_{st} was calculated for each locus.

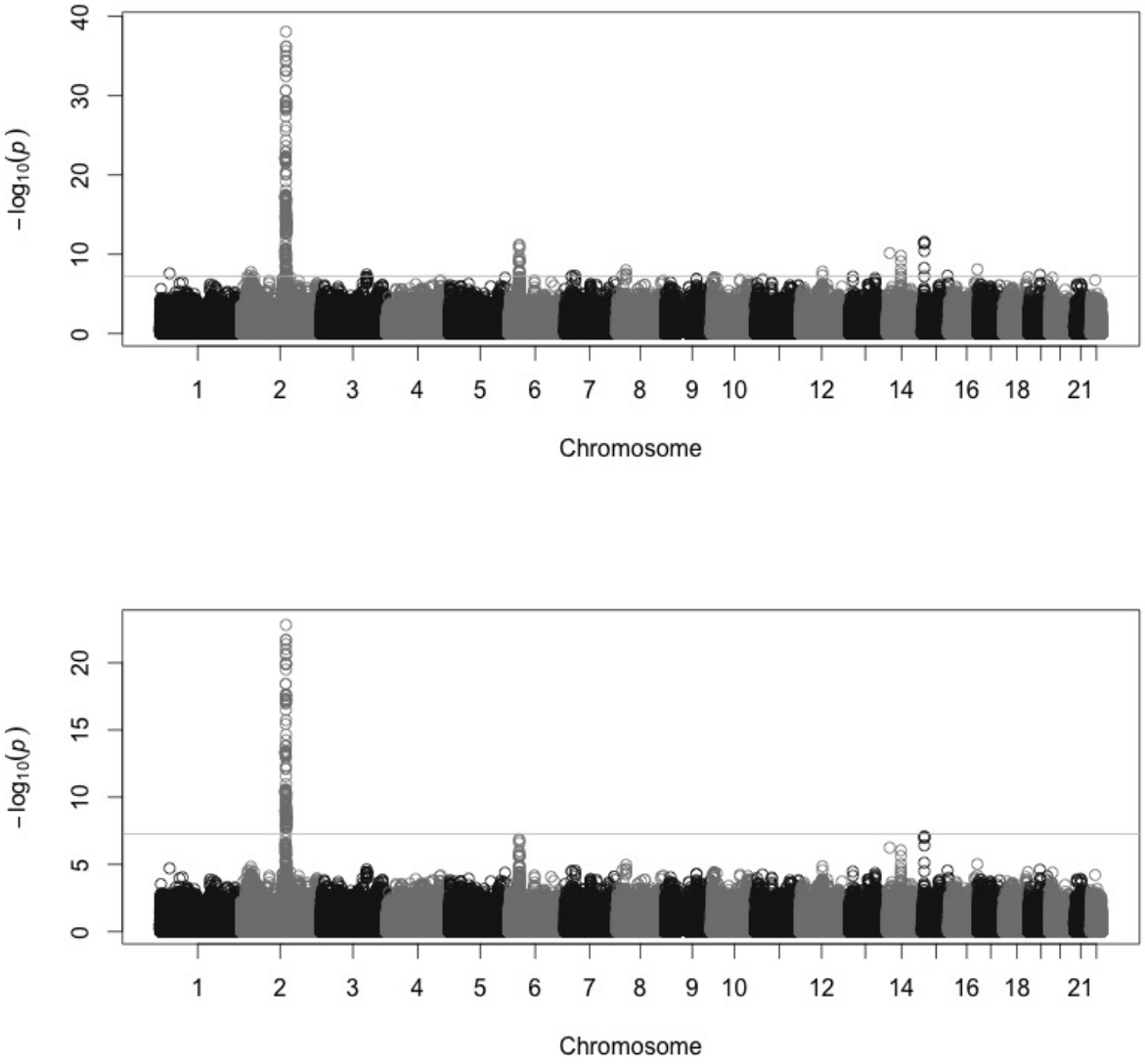

665

666 **Figure 4** EigenGWAS for CEU (112 samples) & TSI (88 samples) from HapMap. a)
667 Manhattan plot for EigenGWAS on E_1 without correction for λ_{GC}. When there was no
668 correction, on chromosome 2 found *LCT*, chromosome 6 *MICA* (HMC region), chromosome
669 14 *HIF1A*, and chromosome 15 *HERC2*. The line in the middle was for genome-wide
670 significant level at $\alpha = 0.05$ given multiple correction. b) Manhattan plot for EigenGWAS
671 on E_1 with λ_{GC} correction, and *LCT* was still significant, and *HERC2* slightly below whole
672 genome-wide significance level. The genome-wide significance threshold was *p*-values =
673 5.44e-08 for $\alpha = 0.05$.

674

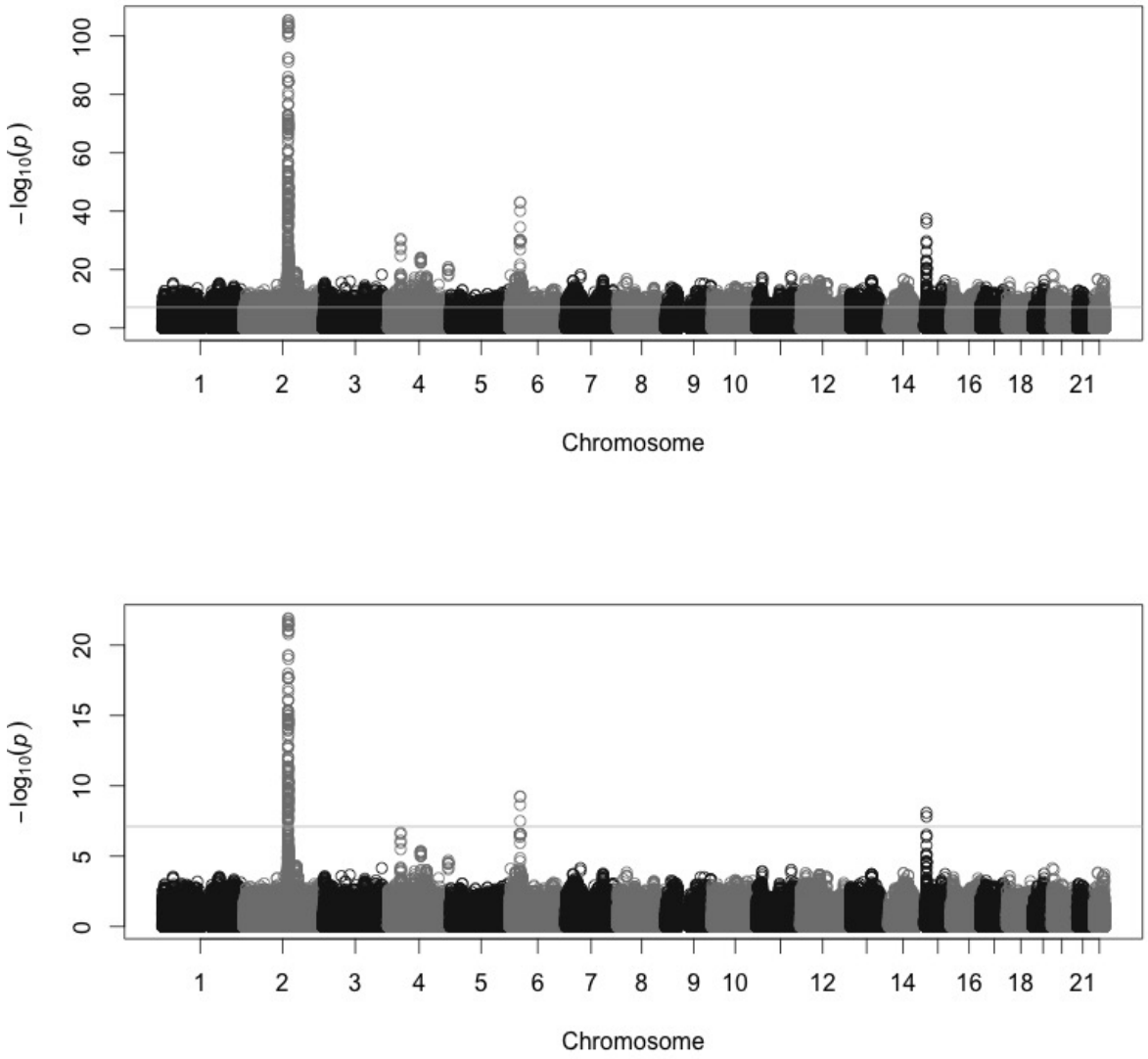

675
676 **Figure 5 EigenGWAS for POPRES samples on eigenvector 1.** a) Manhattan plot for
677 EigenGWAS without correction for λ_{GC}. b) After correction for λ_{GC}, on Chromosome 2
678 found *LCT*, chromosome 6 *SLC44A4*, and chromosome 15 *HERC2*. The genome-wide
679 significance level was *p*-values = 7.76e-08 given $\alpha = 0.05$.
680

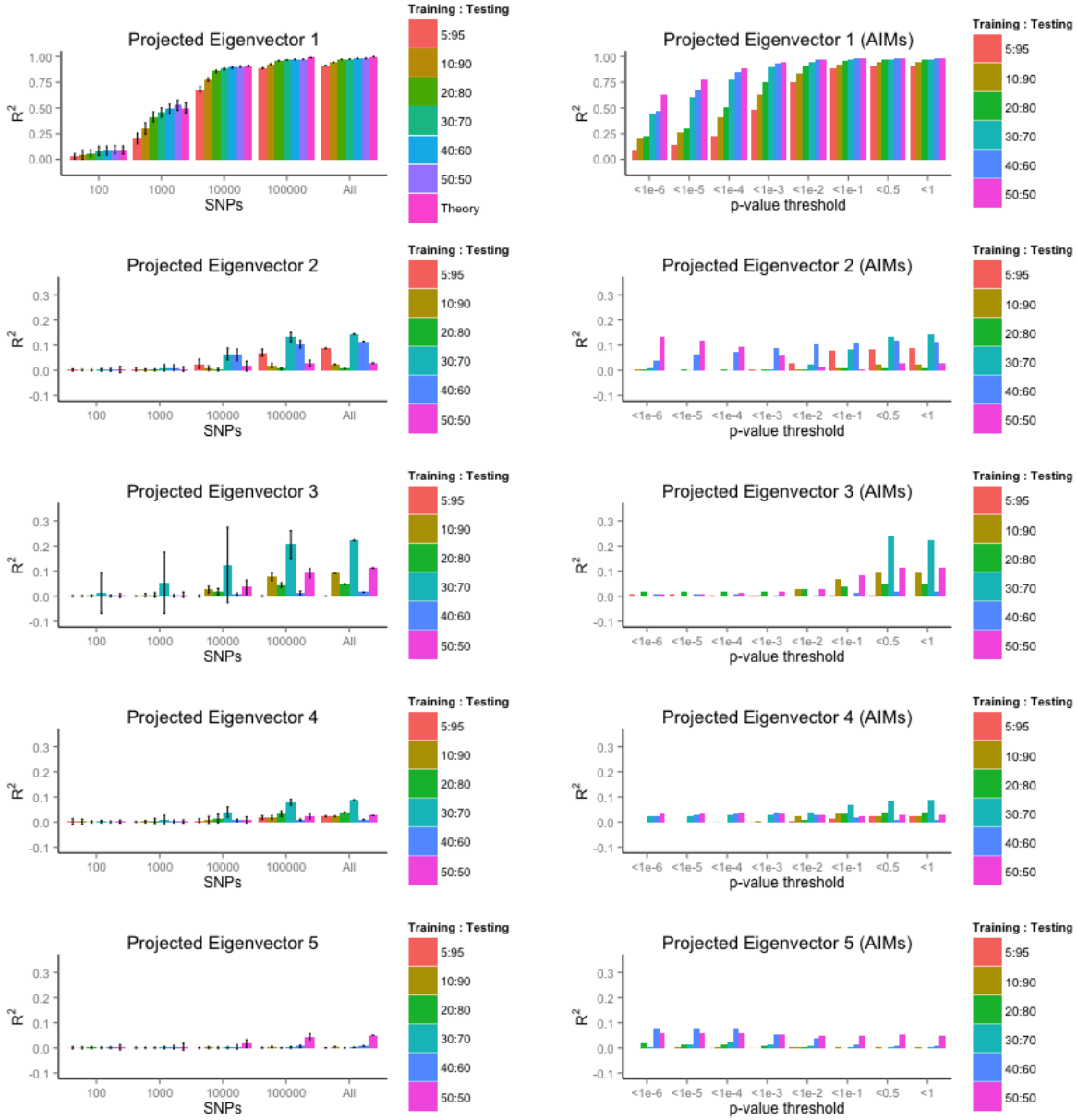

681

682 **Figure 6** Prediction accuracy of the projected eigenvectors for POPRES samples. Given
683 2,466 POPRES samples, the data were split to 5%:95%, 10%:90%, 20%:80%, 30%:70%,
684 40%:60%, and 50%:50, as training and test set. The left columns represent prediction
685 accuracy ( ) using randomly selected numbers (100, 1,000, 10,000, 100,100, all) of
686 markers, the 95% confidence interval were calculated from 30 replication for resampling
687 given number of markers. In contrast, the right columns represent the predicted accuracy for
688 8 p-value thresholds (1e-6, 1e-5, 1e-4, 1e-3, 1e-2, 1e-1, 0.5, and 1) for EigenGWAS SNPs.

689

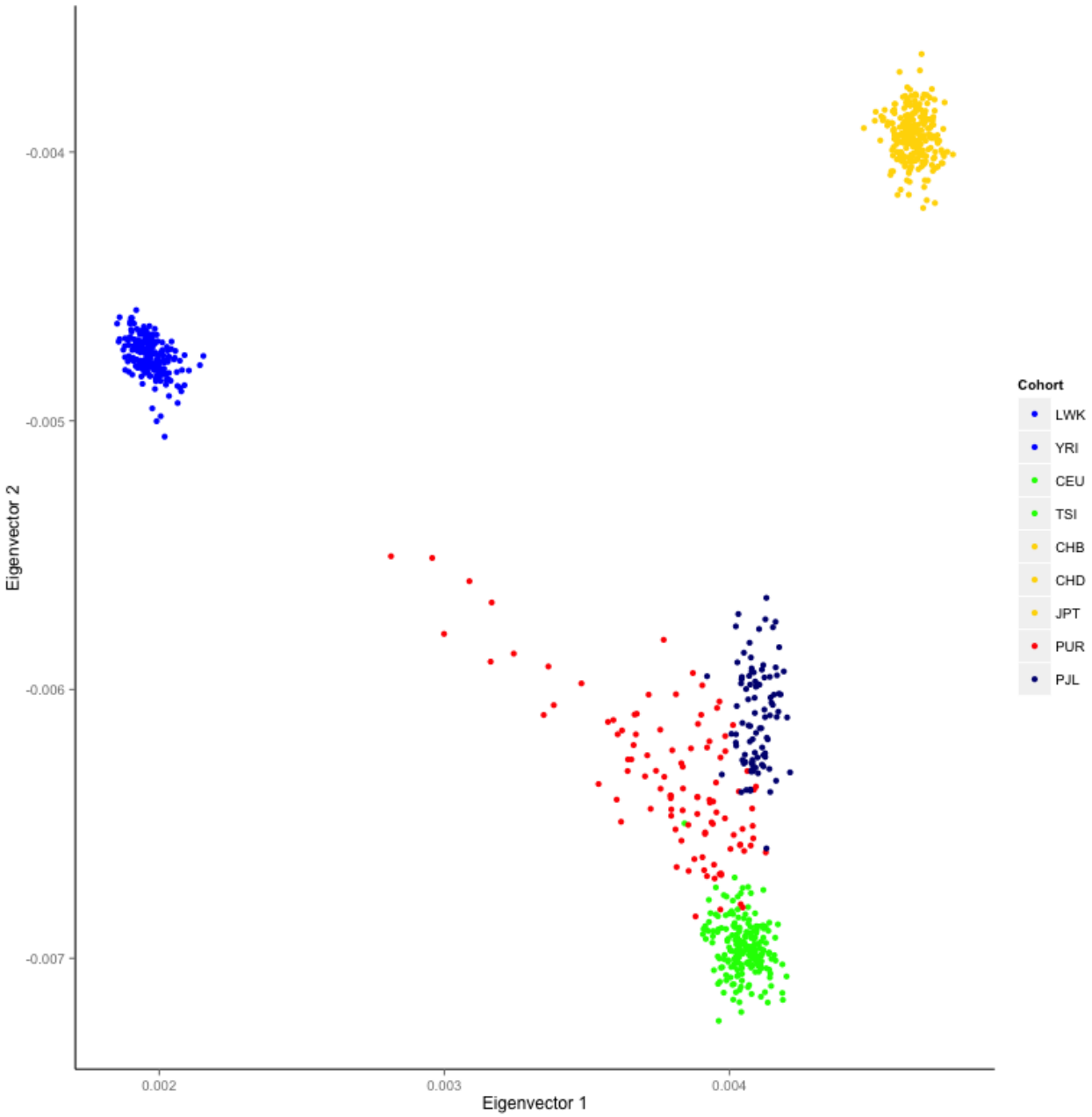

690

691 **Figure 7 Projected eigenvectors for Puerdo Rican cohort (PUR) and Pakistan cohort**
692 **(PJL) in 1000 Genome project**. The training set was HapMap3 samples build on 919,133
693 SNPs. The eigenvectors 1 and 2 for were generated based on the 74,500 common SNPs on
694 chromosome 1. PUR showed an admixture of African and European gene flows, and PJL
695 Asian and European gene flows.
696

Table 1 GWAS signals for on eigenvectors for HapMap and POPRES

	HapMap				POPRES			
Eigenvector (E_i)	Eigen value	GWAS λ_{GC}	#GWAS hits	#After clumping	Eigen value	GWAS λ_{GC}	#GWAS hits	#After clumping
1	100.135	103.715	546,716	231,677	5.104	5.005	10,885	3,004
2	47.658	44.686	382,867	161,022	2.207	1.929	1,254	289
3	7.168	6.471	33,317	15,344	2.157	1.910	1,201	340
4	5.923	5.173	21,935	12,401	2.077	1.464	1,353	331
5	4.402	3.964	9,554	4,727	1.971	1.866	781	76
6	2.449	1.982	1,113	567	1.871	1.295	1,162	111
7	2.285	1.986	593	389	1.843	1.337	1,239	130
8	2.107	1.742	236	171	1.818	1.486	1,259	152
9	2.056	1.729	268	174	1.807	1.503	1,701	113
10	2.0217	1.661	236	163	1.798	1.492	1,639	90

Notes: HapMap has 988 samples, and 919,133 SNPs; its GWAS hits were those had *p*-values < 5.44e-08 given $\alpha = 0.05$. POPRES has 2,466 European samples, and 643,995 SNPs; its GWAS hits were those had p-values < 7.76e-08 given $\alpha = 0.05$.

After clumping, the reported numbers were quasi-independent GWAS hits. Within 250K bp and linkage disequilibrium of $r^2 > 0.5$ only the most significant GWAS hit was counted as a GWAS hit (see PLINK --clump default option).

λ_{GC} was calculated as the ratio between the median of observed χ^2 from EigenGWAS to the median of χ^2 value, which is 0.455.

Table 2 Gene discovery using EigenGWAS

Gene	Lead SNP	Position	Allele	*p*-value (λ_{GC})	MAF (TSI:CEU)	F_{st}	Annotation
CEU & TSI samples							
LCT	rs6719488	2:135817629	G/T	6.68e-34 (1.21e-20)	0.733:0.206	0.558	Lactose persistent locus
DARS	rs13404551	2:135964425	C/T	8.18e-39 (1.51e-23)	0.756:0.206	0.604	Genetic hitchhiking due to *LCT*.
MICA	rs2256175	6:31412672	T/C	8.94e-10 (2.60e-6)	0.665:0.360	0.183	MHC class I polypeptide-related sequence A
HIF1A	rs2256205	14:61670944	A/G	1.51e-10 (8.86e-7)	0.464:0.179	0.192	HIF-1A thus plays an essential role in embryonic vascularization, tumor angiogenesis and pathophysiology of ischemic disease.
HERC2	rs8039195	15:26189679	C/T	2.75e-12 (8.22e-08)	0.403:0.122	0.212	Genetic variations in this gene are associated with skin/hair/eye pigmentation variability
POPRES European samples							
					Southern Europeans : Northern Europeans		
LCT	rs3754686	2:135817629	T/C	3.30e-106 (1.23e-22)	0.514:0.279	0.110	
DARS	rs13404551	2:135964425	C/T	6.32e-102 (8.99e-22)	0.518:0.293	0.106	
SLC4A4	rs605203	6:31819235	C/A	8.94e-44 (5.77e-10)	0.214:0.343	0.040	Defects in this gene can cause sialidosis, a lysosomal storage disease
HERC2	rs1667394	15:26189679	C/T	3.90e-38 (8.15e-09)	0.276:0.173	0.041	

Notes: The *p*-value cutoff for CEU&TSI was 5.44e-08 (919,133 SNPs), for POPRES was 7.76e-08 (643,995 SNPs) at genome-wide significance level of $\alpha = 0.05$. $\lambda_{GC} = 1.725$ for CEU&TSI, and $\lambda_{GC} = 5.00$ for POPRES.

F_{st} is calculated by partitioning the sample into two groups upon $E_1 > 0$. For TSI&CEU set, partitioning on E_1 perfectly separated TSI (88 samples) and CEU (112 samples). For POPRES, partitioning on E_1 separated southern European population (1,092 samples) and northern European population (1,374 samples).